
**Liquid Crystals**
Publication details, including instructions for authors and subscription information:
http://www.informaworld.com/smpp/title~content=t713926090

# The structure of homeotropic smectic C (SmC) alignment within liquid crystal cells

N. Ul Islam; S. J. Elston

Online publication date: 06 August 2010

**To cite this Article** Islam, N. Ul and Elston, S. J.(1999) 'The structure of homeotropic smectic C (SmC) alignment within liquid crystal cells', Liquid Crystals, 26: 5, 709 — 716
**To link to this Article: DOI:** 10.1080/026782999204787
**URL:** http://dx.doi.org/10.1080/026782999204787

LIQUID CRYSTALS, 1999, VOL. 26, NO. 5, 709–716

# The structure of homeotropic smectic C (SmC) alignment within liquid crystal cells

N. UL ISLAM and S. J. ELSTON*

Department of Engineering Science, University of Oxford, Parks Road, Oxford OX1 3PJ, UK

(*Received 24 August 1998; in final form 17 December 1998; accepted 18 December 1998*)

A commercially important ferroelectric liquid crystal, SCE13, is characterized in terms of the parameters of Landau–de Gennes mean field theory and elastic continuum theory. A simple model for the alignment of smectic C (SmC) liquid crystals in cells whose surfaces are treated to cause homeotropic alignment is presented. The expected temperature dependence of the director alignment structures is discussed. Data obtained using half-leaky guided mode techniques are presented in support of this model.



## 1. Introduction

Considerable effort has been expended in recent years on the development of continuum theories for smectic C (SmC) and chiral smectic C (SmC*) ferroelectric liquid crystals (FLCs). This research has been partly motivated by scientific interest, but also by the considerable potential for exploitation of FLCs in display devices [1, 2]. However, there are still hurdles to be overcome if they are to succeed nematic liquid crystals as the display technology of choice. In particular, research has focused on the alignment structures that form within these devices. These are obviously crucial to the optical properties of any display device, and indeed, the multiplexing operating window depends critically on the alignment structures present. Thus it is crucial for the successful design of display devices with controllable characteristics, and for the reliable production of commercially viable displays, that an understanding of the physical processes involved be obtained and the equilibrium structures be modelled.

The director structure most commonly studied has been for homogeneous alignment, where in the SmA phase, the idealized bookshelf geometry has the molecular director, **n**, aligned parallel to the cell surfaces and the layer normal, **a**. However, due to the formation of complicated chevron structures within the bistable SmC and SmC* phases, with their associated hairpin and zig-zag defects for this alignment, it is also useful to make studies of homeotropically aligned cells. Here the layers are taken to be parallel to the cell surfaces, while the director **n** is taken to be perpendicular to them in the SmA phase.

*Author for correspondence.

In recent years, the key optical technique used to probe both this and other alignments has been the half-leaky guided mode (HLGM) technique, pioneered and developed by Sambles and co-workers [3, 4]. This technique, and others [5–8], have been used to extract a variety of ratios of continuum theory coefficients, and to study the behaviour of the structure that forms near the phase transition.

In this paper, we present a continuum theory based model of a homeotropic liquid crystal cell in the SmC phase, use it to determine some of the ratios of these coefficients and study the temperature evolution of the cell surface boundary layers, $z_{bl}$. These boundary layers are regions of localized director realignment near the surfaces of conventional smectic liquid crystal cells, brought about by the (poorly understood) interaction at the liquid crystal–cell surface interface.

## 2. Theoretical background and model

The theoretical approaches to modelling smectic liquid crystals fall into three distinct categories:

(i) Simple phenomenological models based on physical observations;
(ii) Continuum theory based on the symmetry structure of the materials;
(iii) Models allowing for order parameter variation.

The first approach has been used with some success to model switching in FLC devices. For example, Towler *et al.* used it to analyse the combined influences of the spontaneous polarization and dielectric biaxiality, showing the constraints on material parameters required to optimize low voltage, time minimum addressing [9]. The second approach has been most comprehensively

*Journal of Liquid Crystals* ISSN 0267-8292 print/ISSN 1366-5855 online 
http://www.tandf.co.uk/JNLS/lct.htm
http://www.taylorandfrancis.com/JNLS/lct.htm

developed by Leslie and co-workers [10]. Their approach leads to energy density equations with nine terms for the incompressible SmC case (and many more in the compressible case); although complete solutions have so far been found only in a limited number of geometries [11]. The 'simpler' versions of these models of FLCs confined within a conventional cell geometry express the free energy density using a fixed smectic cone angle together with terms describing the surface interaction. This has been extended to include layer compression by Nakagawa, who has used this approach to model 'chevron' structures in homogeneously aligned SmC cells [12].

More complex models use terms describing smectic layer distortion brought about by cone angle variation, along with infinite anchoring at the cell surfaces [6, 13]. These form part of the third approach, which has been developed by Osipov *et al.* [14], Sluckin and co-workers [15], and others.

Due to the difficulty of applying the complete symmetry-based continuum theory to general situations, it is useful to develop simpler 'effective' theories based on the physical properties of materials and devices. These may not allow complete and rigorous modelling of all situations to be performed, but should allow the main observations to be reproduced and allow useful physical predictions to be made. In this paper we consider such a model to describe the statics of homeotropically aligned SmC liquid crystals. The model, essentially part of the third approach, is based on a balance between competing terms describing the contributions to the energy density from various interactions that are thought to be present. Here these are taken to be due to elastic continuum theory (ECT) describing the director structure within the cell and terms from Landau–de Gennes mean field theory (LdG) describing the contribution due to cone angle distortion.



## 3. Energy density expressions

The geometry being considered is illustrated in figure 1. In order to simplify the mathematics, we assume that the smectic layers remain parallel to the cell surfaces and that the director tilt varies solely in the $z$-direction. By considering only solutions where the layers remain parallel, we ensure that the requirement $\nabla \wedge \mathbf{a} = 0$ (where $\mathbf{a}$ is the layer normal vector) is always satisfied. The molecular tilt relative to $\mathbf{a}$ in the SmC phase generally results in a decrease in the layer thickness, which could either lead to a small layer tilt, $\delta$, in order to retain the layer packing density across the cell thickness, or introduce layer dilation stresses. However, in this model we neglect these effects, effectively assuming that either the layers rearrange in the SmC phase, or that the cell thickness decreases appropriately.

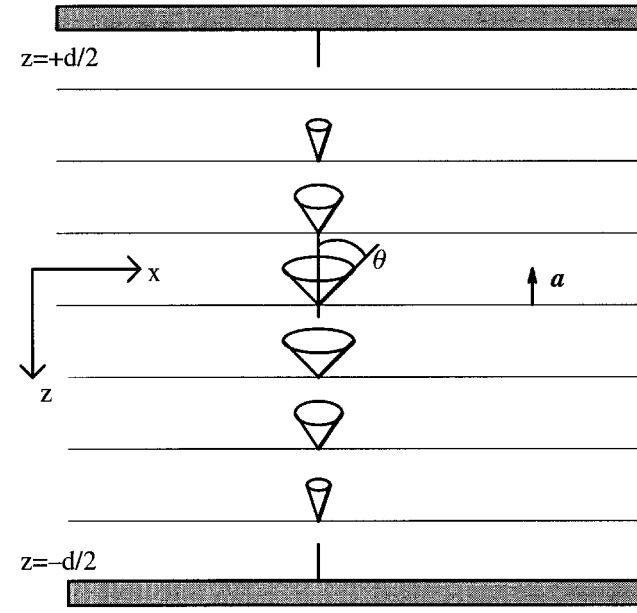


Figure 1. The model of homeotropic alignment used. The cell is of thickness $d$ and the local director tilt (cone angle) is $\theta$. The $z$ coordinate is normal to the cell surfaces, and the layer structure is assumed to be perpendicular to this. Although this is not always so, the results are not significantly affected [14].

Within this geometry we expect the structure that forms to be dominated by two energy density terms:

(i) A term due to the LdG energy of the liquid crystal in terms of the order parameter—the director tilt angle, $\theta$—of the SmC phase, arising from variations away from its equilibrium value,

$$f^{\mathrm{LdG}} = \left(f_0 + \frac{a}{2}\theta^2 + \frac{b}{4}\theta^4 + \frac{c}{6}\theta^6\right) \qquad (1)$$

(ii) A term describing the interlayer coupling using a nematic-like director distortion elastic energy,

$$f^{\mathrm{dir}} = \frac{K}{2}((\nabla \quad \mathbf{n})^2 + (\nabla \wedge \mathbf{n})^2) \qquad (2)$$

where $K$ is the elastic constant and a one constant approximation to the elasticity has been used. In bulk SmC material, the director tilt (or cone) angle is determined by the LdG term.

Near the phase transition, $\theta$ is small and we can neglect terms of $O(\theta^6)$ in the LdG expression. Then we can conveniently re-write it in the form:

$$f^{\mathrm{LdG}} = f_0' + \frac{b}{4}(\theta^2 - \theta_{\mathrm{bulk}}^2)^2 \qquad (3)$$

which is obtained by minimizing the LdG term when $\theta = \theta_{bulk}$, where $\theta_{bulk}$ is the equilibrium director tilt angle within the material, at any given temperature, $T$, in the SmC phase. Within a device in the SmC phase, the surface alignment conditions result in $\theta = \theta_e$ at the cell centre, where $\theta_e$ is determined by the balance between the LdG and director distortion terms. Generally $\theta_e \leqslant \theta_{bulk}$, but away from the SmA to SmC phase transition $\theta_e \cong \theta_{bulk}$, allowing us to work with the natural (and easily observed) $\theta_e$ as a parameter. Additionally, substitution of the director $\mathbf{n} = (-\sin\theta, 0, \cos\theta)$ in equation (2) allows this to be re-written as:

$$f^{dir} = \frac{K}{2}\left(\frac{\partial\theta}{\partial z}\right)^2. \tag{4}$$

The terms (3) and (4) can then be added together to form $f(\theta, \theta_z; z)$, a simple free energy density for SmC material in a homeotropically aligned cell. Minimization of $f$ allows us to write a very simple Euler–Lagrange equation describing the director structure in a SmC cell:

$$K\theta_{zz} + b\theta(\theta^2 - \theta_{bulk}^2) = 0 \tag{5}$$

where

$$\theta_{zz} = \frac{\partial^2\theta}{\partial z^2}. \tag{6}$$

Solving this equation, together with the appropriate boundary conditions (homeotropic surface alignment) allows us to predict the structure present in a cell. Using estimates of the constants $K$ and $b$ in equation (5), allows us to use the solutions to estimate the director structure expected in real cells. The parameter $K$ is associated with distortions in the director structure, and we therefore approximate this with a 'nematic-like' value of $K = 10^{-11}$ N. This is reasonable as the smectic layer density wave is relatively weak, and we therefore expect to have significant molecular interdigitation and a corresponding nematic-like elastic constant. The $b$ term is, to first order, temperature independent, and we use the value measured by Ruan *et al.* for SCE13R of $b = 4 \times 10^4$ Nm$^{-2}$ [16] for our example calculations.

## 4. Solutions

Initially we consider the solution with boundary conditions of $\theta = 0$ at the surfaces ($z = \pm d/2$) and $\theta = \theta_e$ in the bulk. The former condition assumes strong homeotropic anchoring, which we will comment on later. Using the previously stated assumption that $\theta_e \cong \theta_{bulk}$ in the centre of the cell, if we are well below the SmA–SmC phase transition temperature, $T_{AC}$, equation (5) has the analytic solution (in each half of the cell):

$$\theta = \theta_e \tanh\left[\left(\frac{\theta_e^2 d^2 b}{2K}\right)^{1/2}\left(\frac{1}{2} + \frac{z}{d}\right)\right]$$
$$= \theta_e \tanh\left[\left(\frac{\theta_e^2 b}{2K}\right)^{1/2}\left(\frac{d}{2} + z\right)\right] \tag{7}$$

where the parameters are as previously defined. The condition for this to be a reasonable solution (i.e. when $\theta_e \cong \theta_{bulk}$ in the centre of the cell) can now be more rigorously defined as being:

$$\left(\frac{\theta_e^2 d^2 b}{2K}\right)^{1/2} \gg 1. \tag{8}$$

Under this condition, the solution to equation (5) is of a boundary layer form. Over much of the cell thickness, $\theta$ is effectively at (or near) its bulk equilibrium value, but varies rapidly near the surfaces to meet the homeotropic alignment condition. There are two interesting points to note here:

1. The boundary layer solution is independent of cell thickness, as can be seen from the second form in equation (7);
2. The boundary layer thickness, $z_{bl}$, is inversely proportional to the equilibrium tilt angle. Setting the boundary layer thickness as being approximately $z_{bl} = z + d/2$ when the operand in equation (7) is equal to unity, we can write:

$$z_{bl} \cong \frac{1}{\theta_e}\left(\frac{2K}{b}\right)^{1/2} \tag{9}$$

which leads to the values shown in table 1. It is worth noting that for the chosen parameters, the product of $z_{bl}$ and $\theta$ is 0.0224 μm rad; we will return to this later.

It is interesting to note that this boundary layer solution can also be used to estimate the energy contained in the region of distortion. Since the solution comes from a balance between the LdG and director distortion terms, the energy contained in the terms will be of the same order. If in addition we approximate the solution to a linear variation in the boundary region

Table 1. Examples of boundary layer thicknesses for a homeotropic SmC cell.

| $\theta_e$/radians | $z_{bl}$/nm |
|---|---|
| 0.2 | 112 |
| 0.1 | 224 |
| 0.05 | 448 |
| 0.02 | 1118 |
| 0.01 | 2236 |

and $\theta = \theta_e$ elsewhere, we can write:

$$f_{bl} = \int_{bl} K \left(\frac{\partial\theta}{\partial z}\right)^2 dz \approx \frac{K\theta_e^2}{z_{bl}} \approx \theta_e^3 \left(\frac{Kb}{2}\right)^{1/2} \quad (10)$$

which interestingly is of the same form as that presented by de Gennes and Prost for a bend in a smectic phase [17].

Rather than fixing the cell centre boundary condition as $\theta = \theta_e$ it may be more correct to say that the rate of change of director tilt is zero here, i.e. $d\theta/dz = 0$. In this case we can obtain numerical solutions to equation (5) which are presented in figure 2.

This clearly shows that for large $\theta_e$ (i.e. well away from the SmA to SmC phase transition) the solution is 'tanh-like' as shown in equation (7). Also, for small tilt angles, $\theta$, the boundary layer solution breaks down, and the variation becomes smoother, with a 'sin-like' form. This is when the condition represented by equation (8) is no longer satisfied.

Finally, while these solutions are mathematically interesting, it is necessary to consider the effects of finite surface anchoring if predictions for real cells are to be made. In order to do this, we introduce a simple Rapini–Popoular-like surface energy expression of the form:

$$f_{surf} = \frac{1}{2}\alpha_0 \sin^2 \theta_{surf} \quad (11)$$

where $\alpha_0$ is a surface anchoring coefficient and $\theta_{surf}$ is the surface tilt angle. This surface term leads to a surface condition:

$$K(\theta_{surf})_z - \alpha_0 \sin \theta_{surf} \cos \theta_{surf} = 0 \quad (12)$$

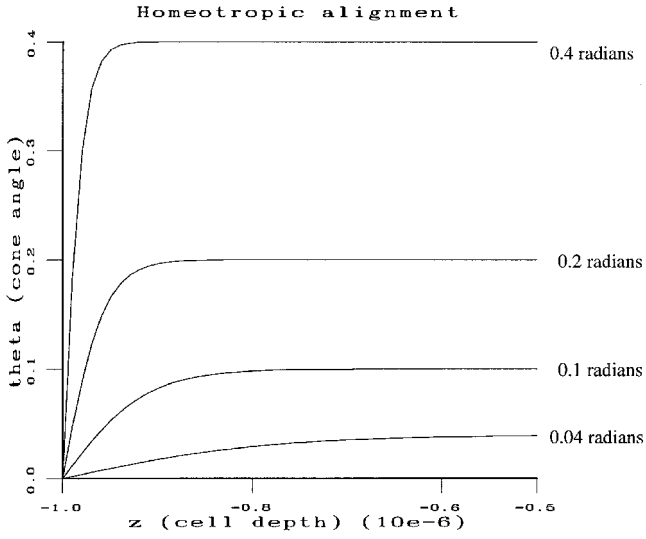


Figure 2. Plots of tilt angle variation for various values of $\theta_{bulk}$. The evolution from a 'sin-like' form to a 'tanh-like' boundary layer profile with increasing $\theta_{bulk}$ (decreasing temperature) is evident.

which replaces the previous homeotropic boundary condition. Solving these equations (5) and (12) together, again numerically, allows the influence of finite surface anchoring to be investigated. This introduces a finite surface tilt, but the functional form of the profile is not affected significantly.

## 5. Experimental details

The experimental set-up is illustrated in figure 3. The set-up consists of incoming s-polarized (transverse electric, TE-mode) light that is incident on the HLGM geometry cell formed from a high refractive index coupling prism, a ferroelectric liquid crystal layer, and a low index float glass substrate. In this set-up there are then a range of incident angles in the coupling prism which excite optic modes in the liquid crystal layer that are bounded at the lower substrate, but not at the upper one. For such modes the distribution of the electric field within the liquid crystal layer is generally quite complex, allowing the use of the polarization mixing in the reflected light to act as a sensitive probe of the director profile [3, 4]. The incoming light source used is a 15 mW He-Ne laser (632.8 nm), and part of the input beam is split off to provide a reference that was used to compensate for any intensity fluctuations of the laser. The depolarization of the reflected light into the p-mode (transverse magnetic, TM-mode) is studied using an analyser with its transmission axis aligned at 90° relative to the input polarization and a photo-diode based detector linked to a computer. The data gathered are then divided by the reference signal in order to determine the absolute depolarization.

The HLGM cell was assembled using 6 μm mylar strips to provide the necessary spacing. Homeotropic alignment was brought about by using the standard

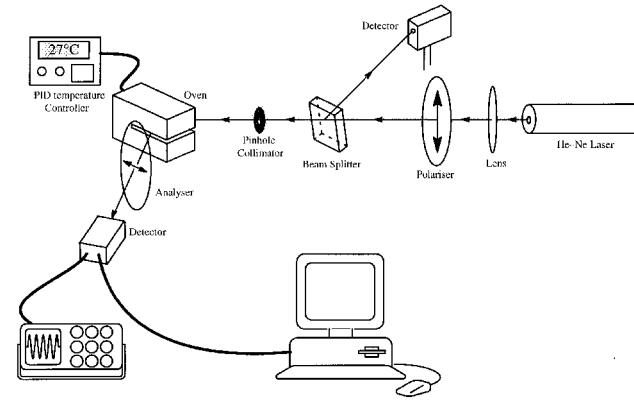


Figure 3. The experimental arrangement used. The HLGM liquid crystal cell is contained in the oven, and the absolute values of $R_{sp}$ are obtained as a function of incident angle. These are corrected for reflections from the prism surfaces, laser beam intensity drift, etc.

technique of drag-wiping with lecithin dissolved in methanol. In addition, during cell fabrication, a pair of transverse electrodes a few mm apart were formed by depositing silver on the substrate. The cell was then capillary filled with SCE13 in the isotropic (I) phase, before being cooled into the SmC* phase. Care was taken when crossing the SmA to SmC* phase transition (in order to form a monodomain layer structure), but once in the SmC* phase the device was cooled quite quickly. Finally, the filled cell was placed in the oven, which was then mounted on a computer-controlled rotation stage.

Data as a function of incident angle were collected from the SmC* and the SmA phases by recording the depolarization as a function of angle. To create sufficiently large domains of uniform alignment within the SmC* phase, a field of $\gtrsim 1\,\mathrm{kV}$ was applied across the 5 mm gap between the transverse silver electrodes, and data were recorded for both positive and negative applied electric fields to check for any bias in the system. An example of the experimental polarization mixing data thus obtained is illustrated in figure 4. Depolarization–incidence angle ($R_{sp}$) curves were obtained for a range of temperatures close to the phase transition temperature, $T_{AC}$.



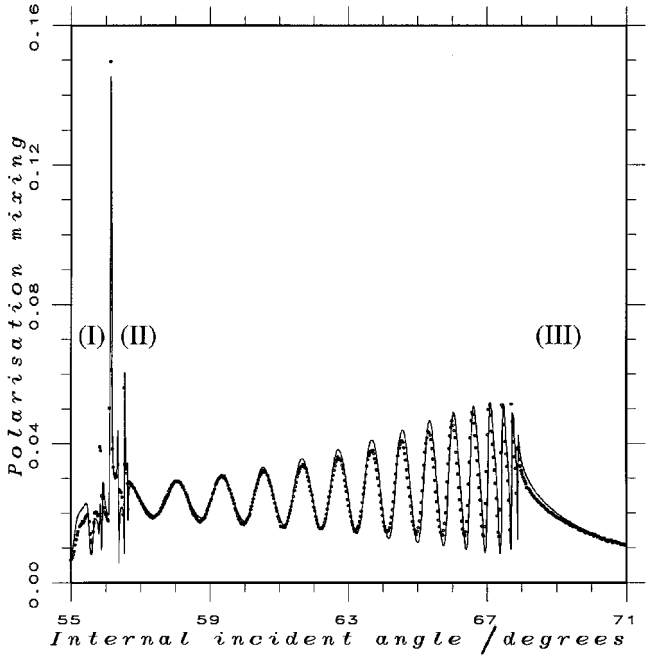


Figure 4. An example of $R_{sp}$ data and the corresponding fit. The data are the individual points and the fit is the continuous line. The quality of the fit is not as good as those in [3, 4, 14, 16, 19, 23] because a strictly limited set of fitting parameters was used.

## 6. Results and modelling

As explained above, the theoretical model is based on the minimization of a free energy density made up of contributions due to the LdG and interlayer coupling energies. This minimization leads to a molecular tilt angle $\theta$ profile which varies smoothly between the bulk value and that at the cell surfaces. It was seen that for $T \ll T_{AC}$ these had a 'tanh-like' form, but for $T \sim T_{AC}$ they were 'sin-like'. This is problematic when comparing data and theory, as there is no simple analytic form which encompasses both regimes. Therefore in order to simplify the data fitting procedure the boundary layer $\theta$-profiles were approximated using sin-curves to describe the variation in those regions, together with a uniform tilt, $\theta_e$, in the 'bulk' of the cell. Taken together with a finite surface pre-tilt, this 'sin-boundary' scheme provides a simple analytic form with adequate levels of approximation to the true profiles over the entire temperature range. The resulting approximated $\theta$-profiles were used in the optical modelling to generate intensity–incidence angle ($R_{sp}$) graphs, using a $4 \times 4$ matrix technique [18].

A further useful feature of modelling the profiles with the 'sin-boundary' scheme is that it provides a direct measure of the boundary layer thickness. Away from the SmA to SmC phase transition, the analytic solution we have given in equation (7) is explicitly 'tanh-like' in form. For this case, the splicing of 'sin-like' boundary layers of equivalent thickness onto an equilibrium value, $\theta_e$, is an adequate representation of the true solution, being accurate to within a few % of the true tilt for all values of the input parameter set. Near the SmA to SmC phase transition, the 'sin-like' form of the solution revealed by numerical modelling is recovered in the use of the 'sin-boundary' scheme by allowing the 'sin-like' layer thickness to tend towards half the cell thickness in this regime.

As can be seen from the data shown in figure 4, there are a number of distinct regions corresponding to the critical angles of the system. It should also be noted that there are certain characteristic features of the $R_{sp}$ curves that are governed by at most a few parameters each. Three interesting regions of the $R_{sp}$ curve shown in figure 4 are marked I, II, III. Region I corresponds to Fabry–Perot modes of the system where the incident angle is less than the critical angle for both the prism–FLC and the FLC–substrate. As the incident angle is increased, the FLC–substrate critical angle is exceeded and region II is entered. This region corresponds to the half-leaky guided modes (HLGMs), where the cell behaves as a wave guide with radiation leaking out at the FLC–prism interface. Further increase in the incident angle results in the prism–FLC critical angle (the 'real' critical angle) being exceeded and region III is entered, where an evanescent field penetrates the FLC boundary

layer region, $z_{bl}$. As the incident angle is further increased, this evanescent 'tail' falls off.

The various boundaries between regions allows the determination of the refractive indices and hence the optical permittivities ($\varepsilon_{\perp}$, $\varepsilon_{\parallel}$, etc). This allows iterative modelling using the other parameters (although further perturbations of the permittivities have to be made). Here these parameters are chosen to be the thickness of the boundary layer, $z_{bl}$, the cell thickness, $d$, the director tilt angle at the surface, $\theta_{surf}$, and the director tilt angle in the 'bulk', $\theta_e$.

The original HLGM technique is predicated on the need to fit the optical depolarization curves to a very high degree of accuracy, due to the large number of parameters in the system. However, as noted above, certain features of the $R_{sp}$ curve are governed by small subsets of the full range of parameters. For example, the height of the sharp mode in figure 4 is largely dictated by the 'strength' of the boundary layer, and therefore how good the wave guiding is in the bulk of the cell. Thus it becomes possible to determine the chosen parameters quantitatively by concentrating on the relevant features of the $R_{sp}$ data. The resulting fits are not of the quality presented by [3, 4, 16], but the parameters used to obtain the fits are determined without ambiguity. One of the major motivations behind the work presented here was the desire to explore the behaviour of the physical structures of the system. Therefore, by concentrating on various features of the $R_{sp}$ curve we could extract information about the parameters that were directly linked to the physical structures ($\theta_e$, $\theta_{surf}$, $z_{bl}$) rather than directly determining the underlying theoretical parameters such as the LdG and interlayer coupling constants.

Taking this approach leads to fits of the form illustrated in figure 4, where adjustments to the parameters (fitting) has been done manually. Extracting the information about the director tilt and the boundary layer thickness from this fitting procedure yields the results shown in table 2. In this the phase transition temperature is 59.6°C, so there is no boundary layer or tilt information at this point. The product of $z_{bl}$ and $\theta$ for each temperature is also shown. This diverges near the phase transition, but away from this point reaches a value of about 0.03 μm rad, compared with our estimate from previous parameters of 0.0224 μm rad.

Table 2. Fitted parameter values for the homeotropic SCE13 cell.

| $T$/°C | $z_{bl}$/μm | $\theta_e$/° | $z_{bl} \times \theta_e$/μm rad |
|---|---|---|---|
| 59.6 | — | — | — |
| 59.4 | 1.90 | 1.20 | 0.040 |
| 59.2 | 1.20 | 1.60 | 0.034 |
| 59.0 | 0.40 | 3.35 | 0.023 |
| 58.4 | 0.33 | 4.95 | 0.029 |
| 57.5 | 0.23 | 6.45 | 0.026 |

Comparison with the results from other work are most convenient in terms of the coefficients in equations (1) and (4). If we note that the leading LdG coefficient can be expressed as $a = \alpha(T - T_{AC})$ and then divide through by $\alpha$, the important coefficients become $b/\alpha$, $c/\alpha$ and $K/\alpha$. These are tabulated, along with the values found by others, in table 3. The results from this work are shown in the first line of the table, where no value of $c/\alpha$ is included due to the simplicity of our approach. The results from the work of Ruan *et al.* [16] are included (where we used $K = 10^{-11}$ N to estimate $K/\alpha$). The results of Yang *et al.* [19] do not allow an estimate of $K/\alpha$ as only the values of the LdG coefficients $b$ and $c$ relative to $\alpha$ are given. The other results given in the table are those from electroclinic effect work [20] and free film work [21]. Clearly the variation in the parameters is not wide, although the results from the free film work are very divergent!

## 7. Discussion and conclusions

Studies of the director profile in homeotropically aligned cells have been made before, but the results appear to be very inconsistent. Mengnan *et al.* used guided mode techniques to study the alignment of the BDH material mix783 on lecithin [22]. In this work boundary layers of around 0.5 μm thickness were observed, although the temperature dependence was not discussed. However studies by Ruan *et al.* for the Merck material SCE13R on lecithin alignment indicated no boundary layer at all [16]. Yang *et al.* have studied the chiral version of the same material and found boundary layers of around 20 nm thickness when using no surface alignment material [19], in which case the anchoring is expected to be very weak. Thus there is apparently considerable variation in

Table 3. Experimentally obtained values of $b/\alpha$, $c/\alpha$, and $K/\alpha$ ($K = K'(\Delta z)^2$).

| Material | $b/\alpha$/K | $c/\alpha$/K | $K/\alpha$/m$^2$ K $\times 10^{-15}$ |
|---|---|---|---|
| SCE13 | 150 | — | 65 |
| SCE13[a] | 241 | — | 60 |
| SCE13[b] | 95 | 500 | — |
| SCE13[c] | 56.6 | 502.2 | 61.2 |
| SCE13[d] | 59 | 240 | 0.28 |
| SCE13[d] | 27 | 133 | 0.85 |

[a] From [16], values obtained using the half-leaky guided mode (HLGM) technique, $K/\alpha$ obtained by estimating $K = 10^{-11}$ N.
[b] From [19], values obtained using the HLGM technique.
[c] From [20], values obtained using the electroclinic effect.
[d] From [21], values obtained using free film studies.

the observed results, even with very similar materials, and the situation needs to be clarified.

Furthermore, the temperature dependence of the boundary layers, $z_{bl}$, needs to be clarified. Osipov *et al.* [14] presented an analysis of homeotropically aligned liquid crystal cells in which the $\theta$-profiles they measured showed boundary layer thicknesses, $z_{bl}$, decreasing with decreasing temperature. This enabled them to measure, in effect, the ratio of the coefficient of elasticity, $K$, to the LdG coefficient $\alpha$. Estimating the phase transition temperature in their work allows the $K/\alpha$ ratio to be approximated for the material SCE8 as $K/\alpha \approx 120 \times 10^{-15}$ m$^2$ K. Their analysis also included the effect of tilted smectic layers within the SmC* phase, but this does not significantly affect the result. Recently, Mazzulla and Sambles [23] studied the homeotropic alignment within an SCE13 filled HLGM cell. They analysed the experimental profiles obtained in terms of a theoretical model put forward by McKay and Leslie [24] which incorporates layer compression explicitly. This allowed them to fit experimental data, yielding $\theta$-profiles that showed the presence of boundary layers. In this case, however, the boundary layers, $z_{bl}$, increase in thickness as the temperature is decreased. This is also in apparent contradiction to the results by Ruan *et al.* which showed no boundary layer [16]. Additionally it is in contradiction to the results which we have presented, which show a boundary layer which decreases in thickness for decreasing temperature for SCE13. This latter result is consistent with LdG theory, and is also consistent with the results of Osipov *et al.* for SCE8 [14]. Further, if the LdG coefficients from [16] are used together with a typical elasticity value, the results are then consistent with ours.

One possible reason for this variation between the results from previous work, particularly [16, 23], may lie in the dearth of discussion about the layer reorganization which must take place in the SmC phase as the temperature is decreased. Having cooled through the phase transition into the SmC phase, the cooling has usually been fairly rapid in previous work [22]. It may be that this is why the results apparently vary, as in practice the smectic layers have to reorganize, and very slow cooling is necessary to ensure that defect-free equilibrium is always achieved. Thus internal stresses created during the smectic layer reorganization may significantly influence the boundary layer structure, and lead to the apparent contradictions.

It should also be noted that the range of temperatures involved in the experiments discussed above does vary. In our work we have studied behaviour close to the phase transition, whereas the work of Mazzulla and Sambles [23], for example, covers a wider temperature range. Different behaviour over different temperature ranges may therefore be a further source of apparent contradictions.

In summary we have presented a simple theory for the director profile in a homeotropically aligned SmC liquid crystal cell. This is based on the balance between the Landau energy term for tilt angle, $\theta$, variation and an elastic energy director distortion term. An analytic solution was obtained for simple boundary conditions which indicated that a boundary layer of tilt variation would be present whose temperature dependant thickness varies inversely with equilibrium tilt angle.

The results from our experiments have indicated the presence of a finite, temperature dependent boundary layer near the surface. Further, results also showed that the behaviour of the thickness of this boundary layer with temperature and tilt angle is consistent with the theory presented. This is not directly consistent with previous results [16, 19, 23], which are also apparently not consistent with each other. However if the results of [16] are combined with a typical elasticity value, then they are consistent with ours. It appears therefore that the results in [23] are particularly mysterious.

The authors wish to thank the following for financial support: the EPSRC, the Royal Academy of Engineering and Sharp Laboratories of Europe (SLE) Ltd. N.U.I., in particular, would like to thank Mike J. Towler of SLE for numerous helpful discussions and Paul A. Gass of SLE for help with the sample fabrication.



## References

[1] Clark, N. A., and Lagerwall, S. T., 1980, *Appl. Phys. Lett.*, **36,** 899.
[2] Elston, S. J., 1995, *J. mod. Opt.*, **42,** 19.
[3] Yang, F., and Sambles, J. R., 1993, *J. opt. Soc. Am. B*, **10,** 858.
[4] Yang, F., and Sambles, J. R., 1993, *Liq. Cryst.*, **13,** 1.
[5] Elston, S. J., and Sambles, J. R., 1991, *Mol. Cryst. liq. Cryst.*, **208,** 1.
[6] Zhuang, Z., Clark, N. A., and Meadows, M. R., 1992, *Phys. Rev. A*, **45,** 6981.
[7] Heinekamp, S., Pelcovits, R. A., Fontes, E., Chen, E. Y., Pindak, R., and Meyer, R. B., 1984, *Phys. Rev. Lett.*, **52,** 1017.
[8] Bahr, Ch., Booth, C. J., Fliegner, D., and Goodby, J. W., 1996, *Ferroelectrics*, **178,** 229.
[9] Towler, M. J., Jones, J. C., and Raynes, E. P., 1992, *Liq. Cryst.*, **11,** 365.
[10] Leslie, F. M., Stewart, I. W., and Nakagawa, M., 1991, *Mol. Cryst. liq. Cryst.*, **198,** 443.
[11] Kedney, P. J., and Stewart, I. W., 1994, *Z. agnew Math. Phys.*, **45,** 882.
[12] Nakagawa, M., 1990, *Displays*, **4,** 67.
[13] Ulrich, D. C., and Elston, S. J., 1996, *Appl. Phys. Lett.*, **68,** 185.
[14] Osipov, M., Sambles, J. R., and Yang, F., 1996, *Liq. Cryst.*, **21,** 727.

[15] VAUPOTIC, N., COPIC, M., and SLUCKIN, T. J., 1998, *Phys. Rev. E*, **57,** 5651.
[16] RUAN, L., SAMBLES, J. R., and TOWLER, M. J., 1995, *Liq. Cryst*., **18,** 81.
[17] DE GENNES, P. G., and PROST, J., 1993, *The Physics of Liquid Crystals* (Oxford University Press).
[18] AZZAM, R. M. A., and BASHARA, N. M., 1987, in *Ellipsometry and Polarized Light* (North Holland, Elsevier Science Publishers BV).
[19] YANG, F., BRADBERRY, G. W., and SAMBLES, J. R., 1994, *Phys. Rev. E*, **50,** 2834.
[20] BELDON, S. M., and ELSTON, S. J., *Liq. Cryst*. (to be published).
[21] UL ISLAM, N., ELSTON, S. J., and TOWLER, M. J., *Ferroelectrics* (to be published).
[22] MENGNAN, G., SAMBLES, J. R., and YANG, F., 1993, *Liq. Cryst*., **13,** 637.
[23] MAZZULLA, A., and SAMBLES, J. R., 1997, *Liq. Cryst*., **22,** 727.
[24] MCKAY, G., and LESLIE, F. M., 1997, *Euro. Jnl. appl. Math*., **8,** 273.